Ultrasensitive, Room Temperature Detection of THz Radiation Using Nonlinear Parametric Conversion

Mohammad Jalal Khan, Jerry C. Chen, Zong-Long Liau, and Sumanth Kaushik

(Invited Paper)

***Abstract*—We demonstrate ultrasensitive, room temperature optical detection of terahertz by using nonlinear parametric upconversion. Terahertz radiation is mixed with pump light at 1550 nm in quasi-phase-matched GaAs crystal to generate an optical sideband or idler wave that is coupled into optical fiber and detected using a Geiger-mode APD. The resulting terahertz detector has a noise equivalent power of 78 fW/Hz$^{1/2}$ with a timing resolution of 1 ns.**

***Index Terms*—Optical frequency conversion, optical phase matching, submillimeter wave detectors, submillimeter wave frequency conversion.**

I. Introduction

Terahertz radiation has attracted a lot of interest in recent years. Its penetrating capability, nonionizing nature, and the fact that many materials have fingerprint spectra at this frequency regime have resulted in increasing use of terahertz radiation for standoff sensing applications like explosive detection [1], penetrative imaging [2], nondestructive evaluation [3], biomedical imaging [4], drug interdiction [5], and vibration sensing [6]. The capability of these systems depends directly on the availability of high-power terahertz sources and ultrasensitive, fast terahertz detectors. Both these technology areas are being actively researched [5], [7]. However, compared to the near infrared, terahertz technology is relatively immature. Commercially available, room temperature direct detectors, like Golay cells and pyroelectric, have poor sensitivities. Other commercial terahertz detectors, like bolometers, are much more sensitive but require liquid helium cooling, and like their room temperature counterparts, have small electrical bandwidths. In contrast, optical detectors are a mature and commercial technology that offers excellent sensitivity with large bandwidths and room temperature operation. Photon multiplier tubes and Geiger-mode APDs (GM-APDs) enable detection down to the single-photon limit at room temperature, with very fast performance [8], [9].

Manuscript received January 31, 2010; revised March 8, 2010; accepted March 9, 2010. Date of publication April 19, 2010; date of current version February 4, 2011. This work was supported by the Office of the Secretary of Defense (OSD)/Director of Defense Research and Engineering (DDR&E) Quick Reaction Fund under Naval Surface Warfare Center Dahlgren Division (NSWCDD) oversight and the U.S. Air Force under Contract FA8721-05-C-0002. Opinions, interpretations, recommendations, and conclusions are those of the authors and are not necessarily endorsed by the U.S. Government.

The authors are with the Massachusetts Institute of Technology, Lincoln Laboratory, Lexington, MA 02420 USA (e-mail: mjkhan@ll.mit.edu; jcchen@ll.mit.edu; liau@ll.mit.edu; skaushik@ll.mit.edu).

Color versions of one or more of the figures in this paper are available online at http://ieeexplore.ieee.org.

Digital Object Identifier 10.1109/JSTQE.2010.2045737

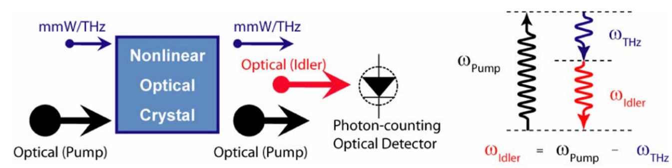

Fig. 1. Terahertz detector concept that leverages optical technologies to perform ultrasensitive, room temperature detection.

As a result, researchers have used various optical pumps and nonlinear crystals to frequency upconvert terahertz waves to optical signals for detection with optical components. Many groups used lithium niobate; their pumps were Nd:YAG [10]–[12] and ti-sapphire [13]. Nd:YAG pumps were also used with $ZnGeP_2$ [14], GaSe [15], and GaP [16] detecting sub-nJ terahertz pulses. At cryogenic temperatures, a group achieved a power conversion efficiency of 4.5×10^{-6} with 1.3-μm pump and GaAs crystal [17]. Recently, a 1.3-μm pump was paired with DAST for terahertz detection [12].

Our scheme to detect terahertz waves leverages telecommunications or 1550-nm technologies to enable ultrasensitive room temperature detection. We employ GaAs, a $\chi^{(2)}$ nonlinear crystal pumped with a readily obtainable erbium-doped fiber amplifier, to parametrically upconvert a terahertz signal to telecomm wavelengths for subsequent detection by an optical detector. Our initial work used a low-cost InGaAsP p-i-n [18]. Subsequently, we used a GM-APD achieving 4.5 pW/Hz$^{1/2}$ noise equivalent power (NEP) with 1 ns temporal resolution [19]. $\chi^{(2)}$ nonlinear interactions are intrinsically very fast; our temporal bandwidth was limited by the optical detector.

In this paper, we improve our previous NEP by over 50 times. This NEP of 78 fW/Hz$^{1/2}$ and power conversion efficiency of 1.2×10^{-3} are the best reported, to our knowledge. Terahertz detection is improved by diffusion bonding and AR coating the GaAs, and by increasing optical pump powers. This paper presents both theoretical and experimental results.

II. Experimental Layout

A schematic representation of a terahertz detector using this technique is shown in Fig. 1. In our study, we have used GaAs as the nonlinear material to perform upconversion. GaAs was chosen because of its high $\chi^{(2)}$ nonlinear coefficient [20] and low absorption losses at terahertz and optical frequencies [21]. Our transmission measurements found losses to be 0.2 and

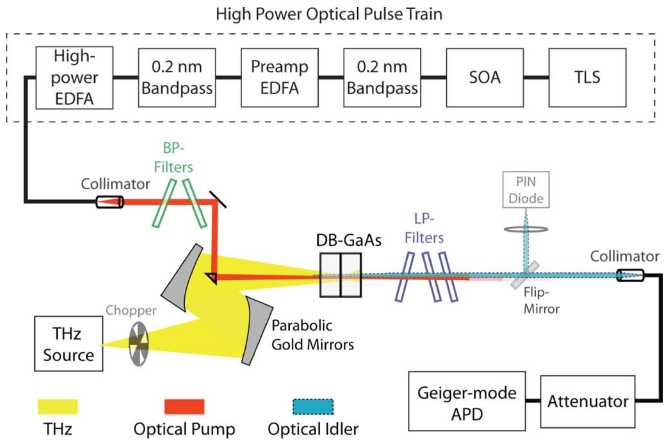

Fig. 2. Experimental layout of terahertz detector.

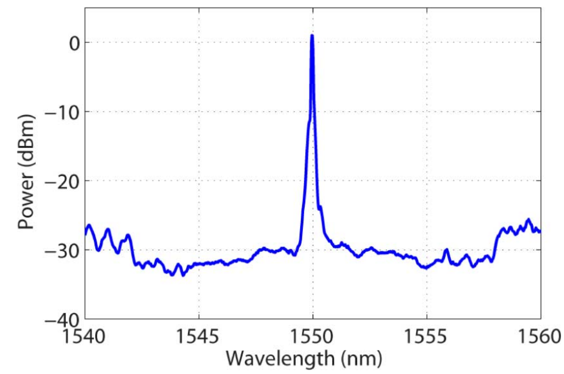

Fig. 3. Optical spectrum of the high-power, pulsed optical pump.

0.065 cm^{-1} at terahertz (0.5–0.7 THz) and optical frequencies (near 193 THz), respectively.

The upconversion experimental layout is shown in Fig. 2. In our experiments, we employed two different terahertz sources. One was a backward wave oscillator (BWO) from Microtech Instruments. The other was Virginia Diode Inc's amplified multipler chain (VDI-AMC). Both terahertz sources produced a tunable, continuous-wave signal. We operated them around the frequency that produced maximum power. For the BWO, this was around 700 GHz, where it provided about 2.5 mW as measured by using a Thomas–Keating power meter. The VDI-AMC was typically operated at 820 GHz, where it produced 120 μW. Although the BWO produces higher power, it is multimoded; by comparison, the VDI-AMC produced a near Gaussian mode, which is more suitable for frequency conversion. The terahertz source radiation was collected and reimaged onto the GaAs crystal by using a pair of 3-in diameter, off-axis parabolic gold mirrors; the crystal position was adjusted such that the beam waist was centered inside the crystal. In our experiments, we employed both bulk and quasi-phase-matched (QPM) crystals. With bulk crystals, the length of GaAs was constrained to the coherent buildup length [22] calculated to be about 4 mm at the operating terahertz frequency based on the reported indices of refraction [21].

Our high-power optical pump source was seeded by an Agilent external cavity tunable laser diode operated at 1550 nm. The 1550-nm light was routed into a semiconductor optical amplifier (SOA) whose supply current was switched with a 10-ns-wide pulse at a 50-kHz repetition rate. The rise and fall time of the SOA was measured to be about 3.5 ns and the resulting pump pulsewidth was about 6.5 ns. The output of the SOA was optically filtered, amplified, and passed through a second filter stage to reduce out-of-band amplified spontaneous emission. Finally, this signal was amplified to the operating power levels by using a high-power, large mode area erbium-doped fiber amplifier (EDFA). The resulting high-power optical source is very flexible and allows easy adjustment of power, pulsewidth, and repetition rate. The typical operating pump power was about 1–2 W average, which corresponds to a 2–4 kW peak power. The optical pump radiation was collimated to a spot size of about 0.9 mm and then passed through two free-space notch or bandpass filters. The filters were each angle tuned for maximum transmission at 1550 nm and had an insertion of loss of less than 1 dB per filter. The filter's 3-dB bandwidth was about 130 GHz with an out-of-band rejection of about 30 dB per filter. This filtering suppressed the optical noise that was produced by the last stage high-power EDFA, enabling easier detection of the idler. The M^2 factor of the last stage power amplifier was about 2. In our experiments, the typical optical pump intensity inside the GaAs crystal was about 200 kW/cm^2. The two-photon absorption coefficient of GaAs at 1550 nm is about 10 cm/GW [22]; consequently, nonlinear absorption does not contribute significantly to material loss until intensities approach 100 MW/cm^2. Our measurements of two-photon absorption in GaAs were consistent with this data. Given the operating pump intensities in our experiments, two-photon absorption effects were negligible. The optical pump was copropagated with the terahertz waves by employing a 5-mm glass prism centered at the second parabolic gold mirror. The small size of the glass prism ensured that the terahertz beam was minimally occluded.

The overlapping terahertz and optical radiation nonlinearly mix in the GaAs to generate the optical idler. The terahertz signal is vertically linearly polarized, whereas the pump is randomly polarized. We used an in-line polarization rotator prior to the last EDFA to maximize the generated idler [23]. The optical idler is then separated from the pump by using three free-space long-pass filters in series. Each filter had a transition band of about 4 nm and a rejection of about 25 dB. The filters were angle tuned to reflect the 1550-nm pump light but to pass wavelengths exceeding 1554 nm. We verified that pump rejection through these three filters exceeded 70 dB; this measurement was limited by detector noise. The idler suffered an aggregate insertion loss of about 4 dB through the filters. We did not make any special effort to separate the terahertz beam from the idler. Since the terahertz beam is a rapidly expanding beam and is not collected by the 1550-nm optics, this was not a concern; additionally, the optical detector is not sensitive to the terahertz radiation. Fig. 3 shows the spectrum of optical source at a resolution bandwidth of 0.1 nm. The optical spectrum was measured coming out of the last stage EDFA. The fiber collimator that sends light to the Ando optical spectrum analyzer (OSA) was purposely misaligned to avoid instrument damage. As can be seen, the optical source has an optical SNR in excess of 25 dB.

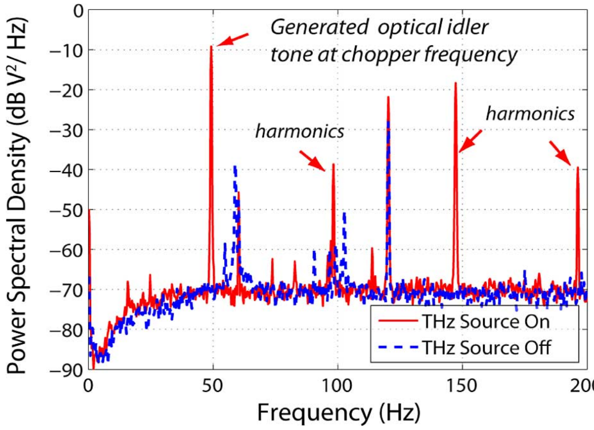

Fig. 4. RF spectrum of New Focus 2153 p-i-n diode output; the optical idler shows up as a clear tone at the chopper frequency.

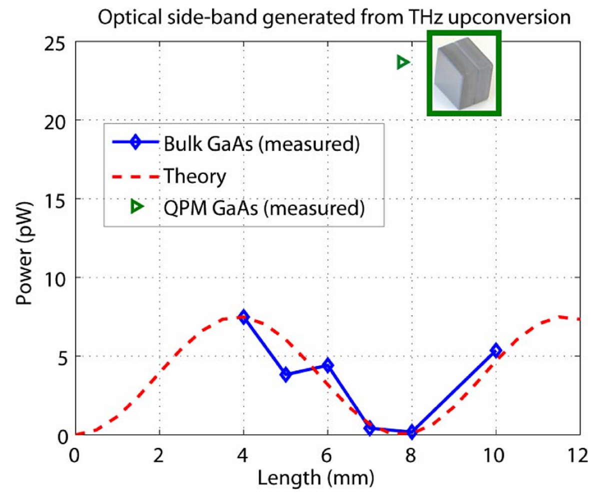

Fig. 5. Optical idler power versus bulk GaAs length; 2-layer QPM GaAs crystal shows a 5 dB improvement over bulk GaAs.

The idler photons can then be coupled either into fiber or routed to a p-i-n diode using a flip mirror. We retained the ability to route the idler beam into a p-i-n diode, as in [18], to enable independent optimization of the upconversion process and coupling of the idler signal into fiber. Initially, the idler generation was maximized by optimally coaligning the terahertz and optical pump beams and then we coupled the idler beam into fiber by removing the flip mirror and using the six-axis fiber collimator. Once in fiber, the idler is routed via a JDS Uniphase switch/attenuator into a Princeton Lightwave GM-APD. Alternately, the light can be coupled into an Ando OSA or to a power meter. The terahertz beam is chopped only when the p-i-n diode is employed; the chopper is removed when idler light is coupled into the GM-APD via the optical fiber.

III. Experimental Results

A. Bulk Versus QPM GaAs

As part of the upconversion optimization, the idler was initially detected using a New Focus 2153 p-i-n diode with an NEP $\approx$23 fW/Hz$^{1/2}$. The terahertz signal was chopped at 49.5 Hz to allow additional discrimination between the generated idler and any remnant pump. The idler power is detected by looking at the p-i-n diode output on an audio spectrum analyzer; alternately, a lock-in amplifier could have been employed. Since the idler is proportional to the product of the terahertz signal and the optical pump, it is produced at the chopper frequency, unlike the unchopped pump. Therefore, any signal at the chopper frequency detected by the diode must correspond to idler power. Fig. 4 shows the electrical spectrum of the p-i-n diode signal. We see a clear spectral tone at the chopper frequency, along with higher harmonics, that together correspond to the idler. To confirm that the harmonics are indeed due to idler power, we turned OFF the BWO, and the tones at the chopper frequency disappeared, as is evident in Fig. 4. The peaks at 60, 120, and 180 Hz correspond to electrical line noise. By integrating the power spectral density (PSD), measured in volts^2/Hertz, over the spectral peak, we can measure the average idler power, given by

$$P_{\text{Idler}} = \frac{1}{R_v}\left[\int_{-f}^{+f} \text{PSD}\, df\right]^{1/2} \quad (1)$$

where R_v is the responsivity of the p-i-n diode in volts/watts.

We measured the idler power produced by bulk GaAs crystals of varying lengths using this technique. Fig. 5 shows a plot of measured idler power versus length. As expected, the conversion efficiency only increases up to the coherent buildup length and then decreases. This is because the optical and terahertz waves walk out of phase such that when the phase difference is π, the idler and the terahertz waves recombine to form the pump. Theoretically, we can estimate the detected power by using the following expression [23]:

$$P_{\text{Idler}} = \frac{8\pi^2 (d_{\text{eff}})^2 L^2 I_{\text{Pump}} T_{\text{Filters}} T_{\text{Fresnel}}}{c\varepsilon_o n_T n_I n_P \lambda_I^2} \times \sin c\left(\frac{\Delta k L}{2}\right)^2 P_{\text{THz}} \quad (2)$$

where d_{eff} is the effective nonlinearity, L is the length of the crystal, I_{Pump} is the pump intensity, and n_T, n_I, and n_P are the refractive indexes at the terahertz, idler, and pump frequencies, respectively. $\Delta k = k_P - k_I - k_T$ is the wave vector mismatch. T_{Filters} is the combined insertion loss of the filters and T_{Fresnel} is the transmission coefficient of the idler at an uncoated GaAs crystal interface. There was excellent agreement between the theoretically calculated idler power and the measured result. For these measurements, the terahertz source was operated at 700 GHz; at this frequency the coherent buildup length is nearly 4 mm based on reported refracted indexes of GaAs [21]. From theory, we expect no upconversion to occur at twice the coherent buildup length; this agrees well with the observed results (see Fig. 5).

The noise performance of the terahertz receiver improves linearly with the terahertz-to-optical conversion efficiency. The conversion efficiency is quadratically related to the length of

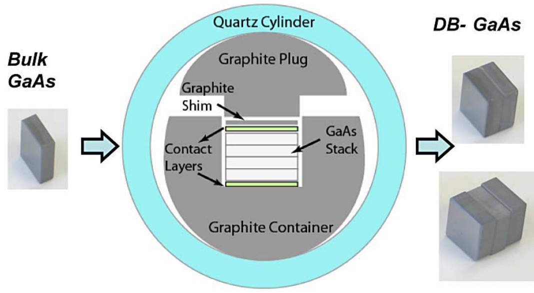

Fig. 6. Diffusion bonding process is used to create QPM GaAs crystals by fusing together two and three orthogonal pieces of bulk GaAs.

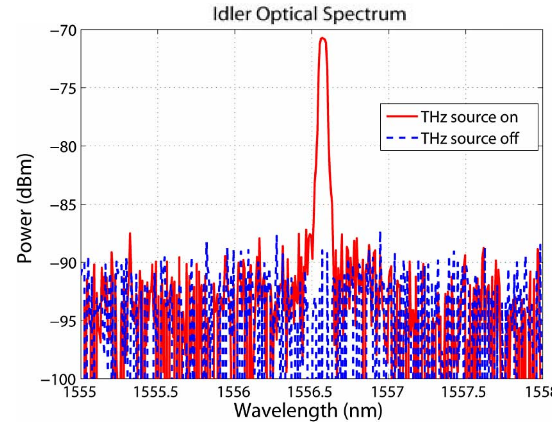

Fig. 7. Optical spectrum of light coupled in the fiber clearly shows the generated optical idler when the terahertz source is on.

nonlinear medium up to the coherent buildup length. To increase the efficiency further, we must overcome the walk off by using specially designed QPM GaAs crystals. A QPM GaAs crystal reverses the polarity of the nonlinearity just as the optical and terahertz beams have slipped out of phase by π radians [23], by stacking alternating orthogonal orientations of GaAs crystal. We fabricated QPM crystals by a diffusion bonding process [24], [25] depicted in Fig. 6. Bulk 4-mm-thick GaAs crystals of orthogonal orientation were put inside a graphite container that was shimmed to tightly fit into a quartz cylinder and then heated to 700 °C. Differential thermal expansion of the graphite and quartz compresses the wafer stack into atomic contact and fuses the GaAs pieces together. The fabrication process was refined to create multilayer GaAs QPM crystals with clean bond interfaces. The exposed surfaces were repolished after the bonding process. Using a two-layer QPM GaAs crystal, we demonstrated a near 5 dB improvement in the conversion efficiency; the theoretical limit is 6 dB (see Fig. 5). We also developed an antireflection (AR) coating at 1550 nm using aluminum oxide and tantalum pentoxide. These materials were specifically chosen because they have low losses at terahertz frequencies. These AR coatings allow more optical pump light into and idler light out of the nonlinear crystal, without absorbing virtually any terahertz. The result is an additional 2.5 dB of improvement in the terahertz-to-optical conversion efficiency.

B. Geiger-Mode APD

After optimizing the conversion efficiency using the p-i-n diode, we coupled the light into the output optical fiber using a matched collimator. Fig. 7 shows the optical spectrum of the output light measured using an OSA at a resolution bandwidth of 0.1 nm. Here, we used a two-layer QPM GaAs crystal AR coated for the 1550-nm optical pump; the terahertz source was the VDI-AMC operated near 820 GHz with an output power of 120 μW. When the terahertz source was turned on, an idler signal appeared at 1556.6 nm, which comes from the nonlinear mixing of the terahertz signal and the 1550-nm pump. Energy conservation dictates that the idler frequency is the difference between the optical pump and the terahertz frequency. For an 820-GHz terahertz signal, we expect an idler exactly at 1556.6 nm as was observed. Conversely, our detection scheme enables the precise determination of the input terahertz wavelength, since the optical pump is well known and the idler wavelength can be accurately measured. The noise floor of the spectrum was limited by the sensitivity of the OSA. We confirmed that at the pump wavelength (1550 nm), no signal was visible above the noise floor. By integrating the power under the spectral peak, we calculated the idler power to be about 85 pW. The terahertz-to-optical photon conversion efficiency is given by

$$\eta_{\text{THz}\rightarrow\text{optical}} = \frac{P^{(p)}_{\text{Idler}}}{P_{\text{THz}}} \times \frac{\nu_{\text{THz}}}{\nu_{\text{Idler}}}$$

where the peak idler power $P^{(p)}_{\text{Idler}}$ is related to the average idler power by the duty factor (20 μs/10 ns). From the OSA measured idler power, we calculate a photon conversion efficiency of 5.9×10^{-6}.

The idler was then routed via an attenuator into the Princeton Lightwave GM-APD [8], which is triggered by a delayed copy of the electrical pulse that drives the SOA. The trigger initiates detection of idler photons in a 1-ns gate by the GM-APD. The GM-APD is equipped with a counter, which records the total number of 1-ns gates with photons over a 1 s time interval. The sensitivity or NEP of the GM-APD is limited by the dark count rate (DCR) or the number of spurious counts per second in the absence of any signal; its sensitivity is given by

$$\text{NEP} = \frac{h\nu}{\eta}\sqrt{\text{DCR}} \qquad (3)$$

where η is the quantum efficiency of the GM-APD, and ν is the frequency of the incident radiation. The DCR of the GM-APD receiver is 20 kHz, which corresponds to an NEP $= 9.3 \times 10^{-17}$ W/Hz$^{1/2}$. To experimentally measure the sensitivity of the terahertz detector, one can attenuate the terahertz power until the counts registered by the GM-APD are equal to the fluctuations in the dark count over the 1 s interval. This attenuated terahertz power would then correspond to the minimum detectable power. Since calibrated terahertz attenuators with a large dynamic range are not readily available, we chose to attenuate the optical idler signal instead. The linear relationship between the idler and terahertz power justifies this approach. Fig. 8 shows a plot of the GM counts as the attenuation of the idler beam was varied. The x-axis values correspond to the equivalent input terahertz power,

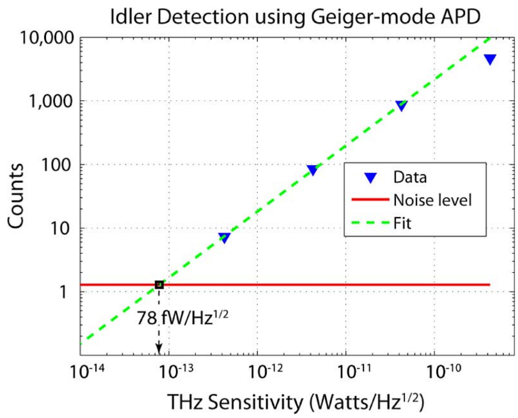

Fig. 8. Plot of GM-APD counts versus input terahertz power normalized by gating signal bandwidth. A linear fit of GM-APD counts (dashed line) intersects noise level (solid line) at 78 fW/Hz$^{1/2}$.

for a given optical attenuation, in units of NEP (W/Hz$^{1/2}$). The *x*-axis values are given by scaling the input terahertz power, 120 μW, by the optical attenuation of the idler, and normalizing it to the square root of the equivalent bandwidth of the gating signal. The equivalent bandwidth of the 1-ns pulse train with a pulse separation of 20 μs and integrated over 1 s is 20 kHz [(20 μs/1 ns) $\times$ 1 Hz]. The mean number of dark counts in 1 s was measured to be 1.6 and was slightly higher than the theoretically expected value of 1 [(1 ns/20 μs) $\times$ DCR]. To calculate the sensitivity of the resulting terahertz detector, we extrapolate a linear fit to the data to the noise level. The fluctuation in the dark counts or noise level is governed by Poisson statistics and is given by the square root of the mean dark counts, 1.6. Using this method, we obtained a terahertz NEP $\approx$ 78 fW/Hz$^{1/2}$, as is shown in Fig. 8. This corresponds to a minimum detectable pulse energy of 1.1 $\times$ 10^{-20} J in the 1-ns GM-APD gate; of course, we integrate over 5 $\times$ 10^4 pulses in 1 s.

The relationship between the NEP of the GM-APD and the resulting terahertz detector is given by

$$\frac{\mathrm{NEP}_{\mathrm{GM\text{-}APD}}}{\nu_{\mathrm{Idler}}} = \eta_{\mathrm{THz}\rightarrow\mathrm{optical}} \frac{\mathrm{NEP}_{\mathrm{THz}}}{\nu_{\mathrm{THz}}} \tag{4}$$

where $\eta_{\mathrm{THz}\rightarrow\mathrm{optical}}$ = (Output idler photons)/(Input terahertz photons) is the system photon conversion efficiency. ν_{THz} and ν_{Idler} are the terahertz and idler frequencies, respectively. Using the aforementioned equation, we calculate the end-to-end receiver photon conversion efficiency of the system to be 5 $\times$ 10^{-6}; the equivalent system power conversion efficiency is 1.2 $\times$ 10^{-3}. These numbers agree very well with the conversion efficiency calculated from the OSA data. The intrinsic photon conversion efficiency is significantly higher and can be calculated by taking into account the 2 dB Fresnel loss at the crystal interface for the terahertz (the crystal is AR coated for optical wavelengths); the 4 dB of insertion losses the idler experiences due to the three long-pass dielectric filters and 4 dB of fiber coupling losses.

Alternately, at a fixed attenuation setting, we can delay the GM-APD's 1-ns gate with respect to the upconverted pulse and thereby measure the idler's temporal characteristics, and thus, infer the terahertz temporal shape. Fig. 9 plots the GM-APD counts versus time. We can see that the upconverted idler signal has a temporal width of about 6 ns. The terahertz source is continuous wave signal, therefore, the temporal shape of the upconverted light mirrors that of the optical pump; the measured pulsewidth agrees well with that of the optical pump, given a 1-ns timing resolution. However, if we had used a pulsed terahertz source, our terahertz detector would provide a 1-ns time-resolved measurement of the terahertz pulse. As is clear from the figure, with the terahertz source OFF, there is no upconverted idler signal; the noise floor of the terahertz detector is only limited by the noise characteristics of the GM-APD, resulting in excellent room temperature detection sensitivity.

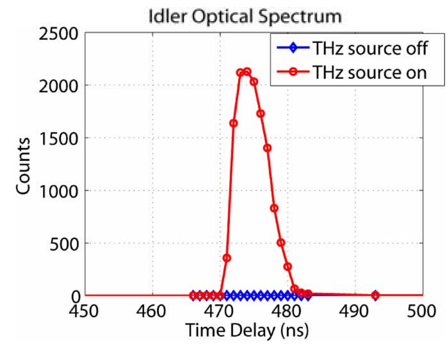

Fig. 9. Idler's pulse shape versus time measured by GM-APD.

IV. Conclusion

We have used optical frequency upconversion at 1550 nm to create a fast, ultrasensitive room temperature terahertz receiver. Nonlinear conversion was enhanced by quasi-phase matching, where two GaAs crystals were diffusion bonded. Increased optical pump powers on these AR-coated crystals resulted in record-breaking power conversion efficiency of 1.2 $\times$ 10^{-3}, which agrees with theory. We show that terahertz can be detected at an unprecedented 78 fW/Hz$^{1/2}$ NEP at room temperature. This sensitivity is nearly 40 dB better than commercial room temperature terahertz detectors and over 15 dB better than commercial 4.2-K bolometers. The detector's temporal resolution is 1 ns.

Acknowledgment

The authors would like thank P. O'Brien of the Massachusetts Institute of Technology Lincoln Laboratory for AR-coated GaAs crystals and for help with imaging the bond interfaces.

References

[1] Y. C. Shen, T. Lo, P. F. Taday, B. E. Cole, W. R. Tribe, and M. C. Kemp, "Detection and identification of explosives using terahertz pulsed spectroscopic imaging," *Appl. Phys. Lett.*, vol. 86, pp. 241116-1–241116-8, Jun. 2005.

[2] A. M. Sinyukov, A. Bandyopadhyay, A. Sengupta, R. B. Barat, D. E. Gary, Z. Michalopoulou, D. Zimdars, and J. F. Federici, "Terahertz interferometric imaging of concealed object," *Proc. SPIE*, vol. 6373, pp. 63730K-1–63730K-8, Oct. 2006.

[3] J. White and D. Zimdars, "Time domain terahertz non destructive evaluation of water intrusion in composites and corrosion under insulation,"

presented at the Quantum Electron. Laser Sci. Conf., Baltimore, MD, May 6–11, 2007, paper JWA112.

[4] E. Pickwell and V. P. Wallace, "Biomedical applications of terahertz technology," *J. Phys. D, Appl. Phys.*, vol. 39, pp. R301–R310, Sep. 2006.

[5] M. Tonouchi, "Cutting-edge terahertz technology," *Nature Photon.*, vol. 1, pp. 97–105, Feb. 2007.

[6] J. C. Chen and S. Kaushik, "Terahertz interferometer that senses vibrations behind barriers," *IEEE Photon. Tech. Lett.*, vol. 19, no. 7, pp. 486–488, Apr. 2007.

[7] P. Siegel, "Terahertz technology," *IEEE Trans. Microw. Theory Tech.*, vol. 50, no. 3, pp. 910–928, Mar. 2002.

[8] X. Jiang, M. A. Itzler, R. Ben-Michael, and K. Slomkowski, "InGaAsP-InP avalanche photodiodes for single photon detection," *IEEE J. Sel. Top. Quantum Mech.*, vol. 13, no. 4, pp. 895–905, Jul./Aug. 2007.

[9] S. Verghese, J. P. Donnelly, E. K. Deurr, K. A. McIntosh, D. C. Chapman, C. J. Vineis, G. M. Smith, J. E. Funk, K. E. Jensen, P. I. Hopman, D. C. Shaver, B. F. Aull, J. C. Aversa, J. P. Frechette, J. B. Glettler, Z. L. Liau, D. C. Oakley, E. J. Ouellette, M. J. Renzi, and B. M. Tyrrell, "Arrays of InP-based avalanche photodiodes for photon counting," *IEEE J. Sel. Top. Quantum Electron.*, vol. 13, no. 4, pp. 870–884, Jul./Aug. 2007.

[10] A. A. Babin, V. N. Petryakov, and G. I. Freidman, "Use of stimulated scattering by polaritons in detection of submillimeter radiation," *Sov. J. Quantum Electron.*, vol. 13, pp. 958–960, Jul. 1983.

[11] R. Guo, T. Ikari, H. Minamide, and H. Ito, "High sensitive detection of THz-wave at room temperature using stimulated polariton scattering in MgO:LiNbO3," *Appl. Phys. Lett.*, vol. 93, pp. 21106-1–21106-8, Jul. 2008.

[12] H. Minamide and H. Ito, "Coherent terahertz-wave generation and detection over a wide frequency range using DAST crystals," *Proc. SPIE*, vol. 7179, pp. 71790C1-1–71790C1-8, 2009.

[13] G. H. Ma, Q. B. Zhu, G. Kh. Kitaeva, and I. I. Naumova, "Narrow-band terahertz wave generation and detection in one periodically poled lithium niobate crystal," *Opt. Commun.*, vol. 273, pp. 549–553, May 15, 2007.

[14] Y. J. Ding and W. Shi, "Observation of THz to near-Infrared parameteric conversion in $ZnGeP_2$," *Opt. Exp.*, vol. 14, pp. 8311–8316, Sep. 2006.

[15] W. Shi, Y. J. Ding, N. Fernelius, and F. K. Hopkins, "Observation of difference-frequency generation by mixing of terahertz and near-infrared laser beams in a GaSe crystal," *Appl. Phys. Lett.*, vol. 88, pp. 101101-1–101101-3, Mar. 2006.

[16] Y. J. Ding and W. Shi, "Efficient THz generation and frequency upconversion in GaP crystals," *Solid State Electron.*, vol. 50, pp. 1128–1136, Jun. 2006.

[17] S. S. Dhillon, C. Sirtori, S. Barbieri, A. de Rossi, M. Calligaro, H. E. Beere, and D. A. Ritchie, "THz sideband generation at telecom wavelengths in a GaAs-based quantum cascade laser," *Appl. Phys. Lett.*, vol. 87, pp. 71101-1–71101-3, Aug. 2005.

[18] M. J. Khan, J. C. Chen, and S. Kaushik, "Optical detection of terahertz radiation by using nonlinear parametric upconversion," *Opt. Lett.*, vol. 32, pp. 3248–3250, Nov. 15, 2007.

[19] M. J. Khan, J. C. Chen, and S. Kaushik, "Optical detection of terahertz radiation using nonlinear parametric upconversion," *Opt. Lett.*, vol. 33, pp. 2725–2727, Dec. 2008.

[20] V. G. Dmitriev, G. G. Gurzadyan, and D. N. Nikogosyan, *Handbook of Nonlinear Optical Crystals.* ser. Springer Series in Optical Sciences 64. New York: Springer-Verlag, 1997.

[21] E. D. Pallik, *Handbook of Optical Constants of Solids*. San Francisco, CA: Academic, 1998.

[22] R. W. Boyd, *Nonlinear Optics*, 2nd ed. San Francisco, CA: Academic, 2003.

[23] W. C. Hurlbut, Y.-S. Lee, K. L. Vodopyanov, P S Kuo, and M. M. Fejer, "Multiphoton absorption and nonlinear refraction of GaAs in the mid-infrared," *Opt. Lett.*, vol. 32, pp. 668–670, Mar. 2007.

[24] Z. L. Liau and D. E. Mull, "Wafer fusion: A novel technique for optoelectronic device fabrication and monolithic integration," *Appl. Phys. Lett.*, vol. 56, pp. 737–739, Feb. 1990.

[25] L. Gordon, G. L. Woods, R. C. Eckardt, R.R. Route, R. S. Feigelson, M.M. Fejer, and R. L. Byer, "Diffusion-bonded stacked GaAs for quasi-phase-matched second-harmonic generation of a carbon dioxide laser," *Electron. Lett.*, vol. 29, pp. 1942–1944, Oct. 1993.

Mohammad Jalal Khan was born in Karachi, Pakistan. He received the S.B., S.M., and Ph.D. degrees in electrical engineering and computer science from the Massachusetts Institute of Technology (MIT), Cambridge, in 1994, 1996, and 2002, respectively. His Ph.D. study has been concerned with integrated photonics for telecommunication optical networks.

He was at Clarendon Photonics as an R&D Engineer, where he was engaged in developing integrated optical devices for the telecommunications industry. He is currently a Technical Staff Member at the MIT Lincoln Laboratory, Lexington, MA, where he is involved in developing active optical systems for sensing and imaging applications. His research interests include using novel nonlinear techniques to detect and generate terahertz radiation.

Dr. Khan is a member of Sigma Xi, Tau Beta Pi, and Eta Kappa Nu. He is a recipient of the Lemelson-MIT Award for innovation in Telecommunications and Networking.

Jerry C. Chen received the B.S.E. degree in electrical engineering and the Certificate in engineering physics from Princeton University, Princeton, NJ in 1989, and the S.M., E.E., and Ph.D. degrees in electrical engineering from the Massachusetts Institute of Technology (MIT), Cambridge, in 1991, 1995, and 1996, respectively.

From 1996 to 1997, he was Postdoctoral Research Fellow at Bell Laboratories, Lucent Technologies, Holmdel, NJ, where he modeled and improved dense wavelength-division multiplexing demultiplexers. Afterward, he performed research on novel optical communication links at the MIT Lincoln Laboratory, Lexington, until 2000. From 2000 to 2002, he was at the Tellabs Research Center, where he was involved in designing and implementing metro fiber networks. In 2002, he rejoined the MIT Lincoln Laboratory, where he was engaged in research on designing and testing laser radar systems, and for the last few years, he has been engaged in research on terahertz receivers and sensor applications. He has coauthored 23 journal articles and holds 9 patents.

Dr. Chen is a member of Optical Society of America, Phi Beta Kappa, Sigma Xi, and Tau Beta Pi and also involved with the Terahertz Technical Program Committee for Conference on Lasers and ElectroOptics of IEEE.

Zong-Long Liau received the B.S. degree in physics from the National Taiwan University, Taipei, Taiwan, in 1972, and the Ph.D. degree in applied physics from the California Institute of Technology, Pasadena, in 1979.

Since December 1978, he has been a Staff Member in the Electro-Optical Materials and Devices Group, Lincoln Laboratory, Massachusetts Institute of Technology, Lexington. He pioneered a mass transport process for semiconductor microstructures, with which he demonstrated a first surface-emitting diode laser array, and a wafer fusion process (also known as direct wafer bonding or diffusion bonding), which has stimulated a wide range of new device applications. Since 2000, he has been engaged in highly powerful microoptics, and has contributed to several laser- and detector-array applications.

Dr. Liau was an Associate Editor for the IEEE JOURNAL OF QUANTUM ELECTRONICS from 1993 to 2002.

Sumanth Kaushik received the B.S., M.S., and Ph.D. degrees in electrical engineering and computer science from the Massachusetts Institute of Technology (MIT), Cambridge, in 1987, 1989, and 1994, respectively.

He is currently the Group Leader of the Space Control Systems Group, MIT Lincoln Laboratory, Lexington. His research interests include advanced technologies in the areas of remote sensing, metrology, and imaging.